

# Vibration control of small horizontal axis wind turbine blade with shape memory alloy

Senthil Kumar Mouleeswaran<sup>1</sup>, Yuvaraja Mani<sup>2</sup>, P. Keerthivasan<sup>1</sup> and Jagadeesh Veeraragu<sup>\*2</sup>

<sup>1</sup>Department of Production Engineering, PSG college of Technology, Peelamedu, Coimbatore, Tamilnadu-641004, India

<sup>2</sup>Department of Mechanical Engineering, PSG college of Technology, Peelamedu, Coimbatore, Tamilnadu-641004, India

(Received September 7, 2017, Revised January 7, 2018, Accepted January 19, 2018)

**Abstract.** Vibrational problems in the domestic Small Horizontal Axis Wind Turbines (SHAWT) are due to flap wise vibrations caused by varying wind velocities acting perpendicular to its blade surface. It has been reported that monitoring the structural health of the turbine blades requires special attention as they are key elements of a wind power generation, and account for 15-20% of the total turbine cost. If this vibration problem is taken care, the SHAWT can be made as commercial success. In this work, Shape Memory Alloy (SMA) wires made of Nitinol (Ni-Ti) alloys are embedded into the Glass Fibre Reinforced Polymer (GFRP) wind turbine blade in order to reduce the flapwise vibrations. Experimental study of Nitinol (Ni-Ti) wire characteristics has been done and relationship between different parameters like current, displacement, time and temperature has been established. When the wind turbine blades are subjected to varying wind velocity, flapwise vibration occurs which has to be controlled continuously, otherwise the blade will be damaged due to the resonance. Therefore, in order to control these flapwise vibrations actively, a non-linear current controller unit was developed and fabricated, which provides actuation force required for active vibration control in smart blade. Experimental analysis was performed on conventional GFRP and smart blade, depicted a 20% increase in natural frequency and 20% reduction in amplitude of vibration. With addition of active vibration control unit, the smart blade showed 61% reduction in amplitude of vibration.

**Keywords:** active vibration control; smart blade; Nitinol [NiTi] wire; SHAWT; flapwise vibration

## 1. Introduction

With wind turbine blades being the key element in the power production of a wind turbine system. Continuous monitoring of the structural health of the wind turbine blade system has provided knowledge on different conditions under which the blades are excited. Recent studies of Arrigon *et al.* (2011) also indicate that blade damage was the most expensive type of damage to repair and can cause serious secondary damage to the wind turbine system due to flap wise vibrations. The natural frequencies are critical component of a given structure. If a force with a similar frequency acts on the structure, it can cause catastrophic failure by increasing the deflections and accelerations.

The mode shape of the structure was also to be replicated by the propagation of the applied force. As the forcing frequency matches with the natural frequency of the blade system, resonance occurs causing severe failure of the blade system. Thus the structure must be designed in such a way to avoid the occurrence of resonance and if the resonance cannot be avoided, then it should have a facility of damping it away by reducing the vibrational velocity levels so as to cause minimum damage to the components, as depicted by Ehsan *et al.* (2012). An alternative to this approach was implementation of shape memory alloy actuator wire in rotor blades of domestic wind turbines, as

presented by Qiao *et al.* (2012). A domestic horizontal axis wind turbine blade has the flat side of the blade facing absolutely into the wind because it has no pitch control inbuilt in it which causes more flap wise vibration of the small wind turbine blades.

Ehsan *et al.* (2012) observed that the first bending mode that plays a crucial role in generating vibration and noise. Hence in this work, the flapwise vibration, i.e., first natural frequency of the blade will be targeted and the impact of SMA based vibration control methodology used here on flapwise vibration will be briefed. These flapwise vibration will be transmitted to the structure and then to the ground. Propagation of vibration of blade to structure, at resonant condition could induce vibration at various parts of the structure. In extreme cases, vibration of the blade can cause damage to buildings, as suggested by Arrigon *et al.* (2011).

Smart materials possess super elasticity nature and hence used in wide range of applications in real time scenario. Bhargav *et al.* (2013) suggested smart materials available in the form of Shape Memory Alloys [SMA] possess good thermo-electric property which can be used for active vibration control in practical applications. These Shape Memory Alloys are used in the form of Nitinol [NiTi] wires in composite shafts in order to effectively control the vibration phenomenon. Nitinol wires embedded within these composite shafts also provide good stiffness characteristics, which enhances better vibration control, which was concluded by Gupta *et al.* (2011).

Yuvaraja *et al.* (2013) presented that Shape Memory Alloy are also used as spring based dynamic vibration absorber with the help of microcontroller in cantilever beam

\*Corresponding author  
E-mail: Jagan047@gmail.com

for better vibration control. The epoxy resin composites filled with NiTi alloy short fibers and particles which were fabricated and their mechanical properties were investigated. Due to the addition of SMA fillers, the flexural rigidity of SMA/epoxy composites increased as shown by Terako *et al.* (2004). GFRP beam was modeled in cantilevered configuration with externally attached SMAs and piezoelectric patches. The results of Yuvaraja *et al.* (2013) revealed that, vibration characteristics of GFRP beam was more effective when SMA was used as an actuator.

Characterization of SMA wires will be performed, to obtain the empirical relation between the current supplied and the deflection thus obtained on the wires. With the empirical relation providing the necessary actuation parameters for the active vibration control, a current control unit will be developed. Harmonic analysis will be performed on conventional and SMA wire embedded smart blade. Under both with and without current control kit, active and passive respectively, the experiment will be conducted and the results will be discussed. The effect super elastic and shape memory nature of SMA and its impact on vibration control in the wind turbine blades will be detailed.

## 2. Development of smart blade

A set of Glass Fibre Reinforced Polymer (GFRP) blade, one conventional and another embedded with NITINOL (NiTi) SMA wire in between the top and bottom layers have been manufactured with the help of die as shown in the Fig.1.

The die which was also made up of GFRP was acquired from the manufacturer and used for hand layup process. Four Glass fibre CSM Mats (300 GSM) are used with volume fraction of 60%. The blade manufactured was of 1.1 m length and weighing about 1.4 kg. Four SMA wires of 0.5 mm diameter and length 180 mm are embedded along the length of the blade.

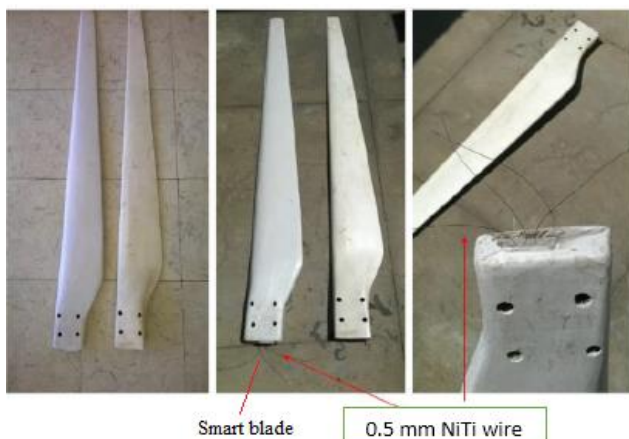


Fig. 1 Conventional and smart wind turbine blade

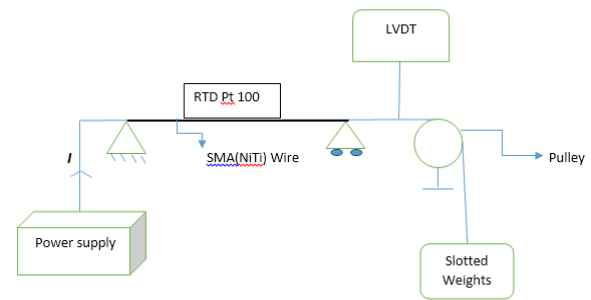


Fig. 2 Experimental setup for determination of Nitinol [NiTi] SMA wire characteristics [Block Diagram]

## 3. Actuation of SMA

Shape-memory alloys (SMAs) generally possess sensing and actuating functions. Smart or intelligent composites can be formed by embedding SMAs into composite materials. The studies reveal about the commercially available SMAs, NiTi alloys – in the form of wires, ribbons or particles which are widely used because of their excellent mechanical properties and shape-memory performance. Kazeem *et al.* (2014) depicted that these materials have found application in broad fields of engineering and science as a result of their superior thermo mechanical properties. NiTi SMAs are used in applications such as vibration control, position control and adaptive stiffening.

### 3.1 Characteristics study of SMA

In order to study the pseudo-elastic nature of SMA, the above was electrically heated above its transformation temperature by supply of current, considerable mechanical force was exerted due to its phase transformation as suggested by Bhargav *et al.* (2013). The experimental study of Nitinol [NiTi] SMA wire under different load conditions along with varying current are observed as shown in the Fig. 2 and the corresponding temperature as well as respective displacement are noted with the help of NI LabVIEW 2015 software.

Nitinol [NiTi] SMA wire of 0.5 mm diameter and length of 180 mm purchased from M/S Dynalloy Inc. was used for this experiment. The Austenite Transition temperature of Nitinol wire is 90°C. The loading values chosen were 0.25 kg, 0.55 kg, 0.75 kg. The current was varied from 1 A to 2.5 A with a step of 0.25 A. Graphs are plotted between current (A), temperature (°C), and displacement (mm) for better understanding.

The experimental set up for determination of Nitinol [NiTi] SMA wire characteristics consists of Nitinol [NiTi] SMA was held between G-Clamp with pulley and fixed support as shown in the Fig. 2. Weighted slots of 0.25 kg, 0.55 kg and 0.75 kg are hung over the pulley for loading conditions. Resistance Temperature Detector [RTD Pt100] was placed at the midspan of Nitinol [NiTi] SMA to detect the temperature under different loading conditions as the current was being supplied from the power supply. One end of the SMA wire was connected with the Linear

Variable Displacement Transducer [LVDT] to determine the displacement produced under various loading conditions.

Similarly, experimental observations were carried out for stress values of 27.47 MPa and 37.47 MPa. The relationship between temperature ( $^{\circ}\text{C}$ ) Vs displacement (mm) and current (A) vs displacement (mm) were shown in the Figs. 3 and 4 respectively.

From the Fig. 3, it can be inferred that, maximum displacement of 6.8 mm was obtained for the temperature of  $81^{\circ}\text{C}$ , when a stress value of 12.49 MPa was applied and current of 2.5 A was supplied. The Austenite Transition temperature ( $T_A$ ) of Nitinol (NiTi) wire of diameter 0.5 mm was  $90^{\circ}\text{C}$ . Since, the maximum temperature of  $86^{\circ}\text{C}$  for stress value of 37.47 MPa was less than the Austenite Transition temperature ( $T_A$ ), the super elasticity nature of SMA wire holds good during the process of experimentation.

Table 1 Experimental observations for 12.49 MPa Stress

| Stress (MPa)                       | 12.49 |     |      |     |      |     |      |     |
|------------------------------------|-------|-----|------|-----|------|-----|------|-----|
| Deflection(mm)                     | 0.5   | 2.9 | 4.7  | 5.8 | 6.3  | 6.5 | 6.7  | 6.8 |
| Current(A)                         | 0     | 1   | 1.25 | 1.5 | 1.75 | 2   | 2.25 | 2.5 |
| Temperature ( $^{\circ}\text{C}$ ) | 29    | 37  | 45   | 50  | 57   | 65  | 74   | 81  |
| Time Taken for Heating (s)         | 0     | 124 | 134  | 143 | 160  | 171 | 174  | 189 |
| Time Taken for Cooling (s)         | 0     | 191 | 210  | 225 | 257  | 263 | 277  | 297 |

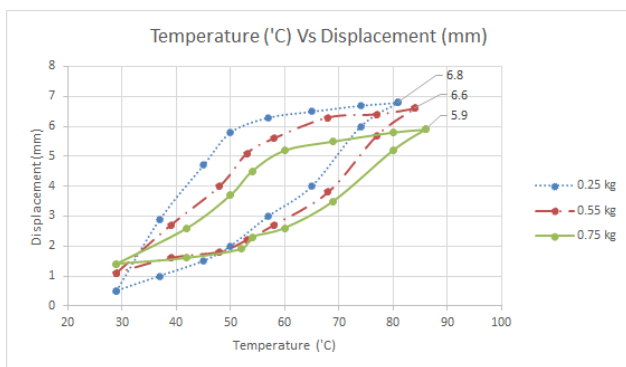


Fig. 3 Comparison of Temperature ( $^{\circ}\text{C}$ ) Vs Displacement (mm) for different loads

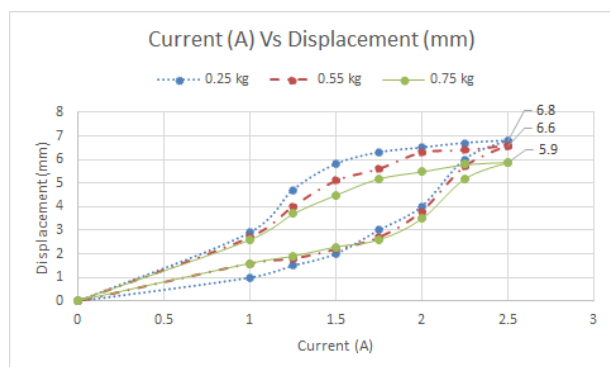


Fig. 4 Comparison of Current(A) Vs Displacement (mm) for different loads

From the Fig. 4, it can be inferred that, among the three different loads, maximum displacement 6.8 mm was obtained, when a stress value of 12.49 MPa was applied and current of 2.5 A was supplied. Whenever the current was supplied to the SMA wire, the wire contracts on heating and expands on cooling when the supply of current was stopped. Equations for displacement (mm) Vs current (A) were established from the experimental study are shown below for the stress value of 12.49 MPa

$$I = 0.0367d^3 - 0.3906d^2 + 1.3969d - 0.613 \quad (1)$$

where, I = Current (A) and d = Displacement (mm)

Since, the stress value of 12.49 MPa provides maximum displacement of 6.8 mm at a temperature of  $81^{\circ}\text{C}$ , the cubic equation corresponding to the stress value was chosen and fed into the active current controller unit.

#### 4. Vibration control in SHAWT blade

Shape Memory Alloy with the help of microcontroller was studied for varying frequencies in case of cantilever beam. The tested results show that the performance of SMA based actuator was capable of controlling the amplitude of vibration for varying excitation frequencies was experimented by Yuvaraja *et al.* (2013). Self-tuning pole placement control for active vibration of a flexible beam has been analyzed. The vibration was controlled using a piezoelectric actuator bonded on a flexible beam by Saad *et al.* (2015). Active damping in vibration with nearly 90% of reduction in vibration amplitude has been done experimentally by Jovanovic *et al.* (2013) for an active vibration control system of aluminium plate with piezo-ceramic patches. Smart structure technology has been employed by Lin *et al.* (1999) using piezoelectric sensor in rotor blade tip which suppressed 85% of structural vibration and was considered satisfactory. A proportional-derivative control for minimizing the blade root load variation in the flapwise direction was successfully done through experiment and 20%–30% reduction in the oscillations of blade root load from the mean value was achieved by Lee *et al.* (2014). Bending and torsional vibrations in flexible cantilever plates are reduced by using nonlinear controllers with piezo-electric sensors experimentally by Qiu *et al.* (2015). PID based active vibration control system was successfully implemented in cantilever beam by Khot *et al.* (2012). An adaptive-passive dynamic vibration absorber with SMA springs was developed by Mani *et al.* (2015) to reduce vibration at various frequencies.

##### 4.1 Development of electronically piloted current controller unit

The electronically piloted current controller unit was fabricated for active control of flapwise vibrations existing in the Small Horizontal Axis Wind Turbine [SHAWT] blades. When the wind turbine blades are subjected to varying wind velocity, flapwise vibration occurs frequently which has to be controlled continuously, otherwise the blade will be damaged due to the resonance phenomenon.

Therefore, in order to control these flapwise vibrations actively, an electronically piloted current controller unit was developed and fabricated. The block diagram of electronically piloted current control unit is shown in the Fig. 5.

The electronically piloted current controller unit has two ports. The first port is used for connecting the current controller unit with the 230V AC power supply through power cable. The second port was used to connect the current controller unit with the personal computer via USB cable. The positive and negative terminals of the current controller unit are connected with SMA wires embedded within the smart wind turbine blade. Uniaxial acceleration sensor OG3225F2 was placed near the tip of the smart blade to sense the acceleration induced by the blade at various frequencies. The DAQ 9234 connects personal computer and the uniaxial acceleration sensor which was linked in channel 2. Once the power supply was switched on, the closed loop activates and the LABVIEW program in the personal computer displays the displacement, maximum RMS value and current required to reduce the displacement. Corresponding load current and voltage are displayed in the panel meter of the current control unit. The electronically piloted current controller unit is shown in the Fig. 6.

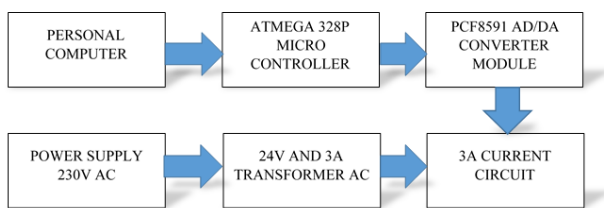


Fig. 5 Block diagram of electronically piloted current controller unit

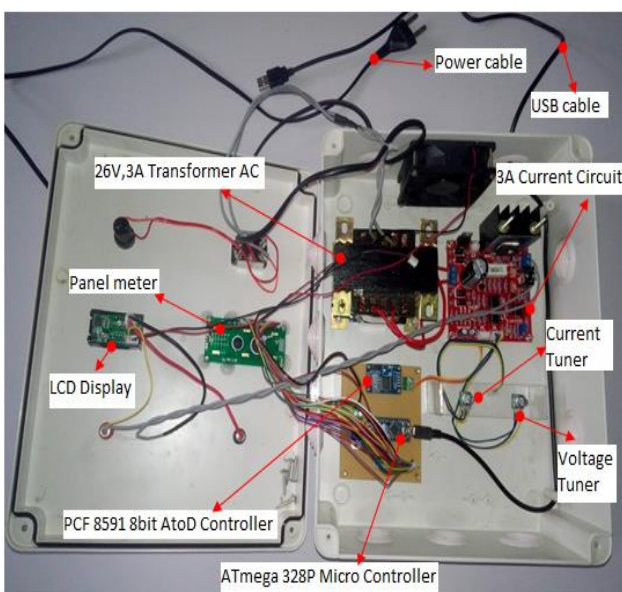


Fig. 6 Electronically Pivoted Current Controller Unit

The electronically piloted current controller unit also consists of ATmega 328P Micro Controller, PCF 8591 8-bit Analog to Digital (A/D) and Digital to Analog (D/A) converter, 24V and 3A Transformer AC, 3A Current Circuit and an exhaust fan which acts as a cooler to remove excess amount of heat generated within the controller unit. The ATmega 328P Micro Controller was commonly used in autonomous systems where a simple, low-powered, low-cost micro-controller was needed. The most common implementation of this chip was on the popular Arduino development platform, namely the Arduino Uno and Arduino Nano models.

The PCF8591 AD/DA Analog-Digital-Analog Converter Module was used for converting the analog signals obtained from the acceleration sensor into digital values representing the displacement of the blade. The 24V, 3A step down transformer AC was used for reducing the 230 V from the power supply to 24 V required in the current control unit. 230 V power supply was supplied to the controller unit through power cable.

## 5. Harmonic analysis

Sellami *et al.* (2016) performed modal and harmonic analysis of three dimensional micro turbines and the dynamic behaviour at different operating frequencies were determined. Natural frequency and damping ratio were calculated for cantilever beam with acceleration sensor placed at the tip of the beam by experimental vibrational analysis and the results were concluded by Singh *et al.* (2017). Tushar *et al.* (2014) performed Experimental and numerical vibration analysis of piezo-laminated cantilever beam and the numerical results closely agree with the experimental results. Lower order harmonic frequencies of flexible beam were detected using piezo-electric accelerometer through frequency domain analysis by Feng *et al.* (2005). The first bending mode's nature in generating vibration and noise was explained by Ehsan *et al.* (2013), hence explained controlling that mode of the wind turbine blade was priority.

### 5.1 Experimental harmonic analysis

Experimental harmonic analysis for passive vibration control was performed on SMA (NiTi) wire embedded wind turbine blade to determine the maximum deflection of blade at different frequencies varying from 10 Hz to 128 Hz. This analysis was performed to observe how the blade vibrates at resonant frequency of 25 Hz. The frequency (Hz) Vs displacement (mm) for passive vibration control in smart blade shows that the maximum displacement was found to be 8.6 mm for the frequency of 30 Hz.

The first, second and third natural frequency obtained from the generated FRF curve by experimental modal analysis was 25 Hz, 60 Hz and 114 Hz respectively for conventional wind turbine blade. The experimental setup for active vibrational control in SMA embedded blade was shown in the Fig. 6. The uniaxial accelerometer sensor was placed on the blade tip to sense the flapwise vibrations and

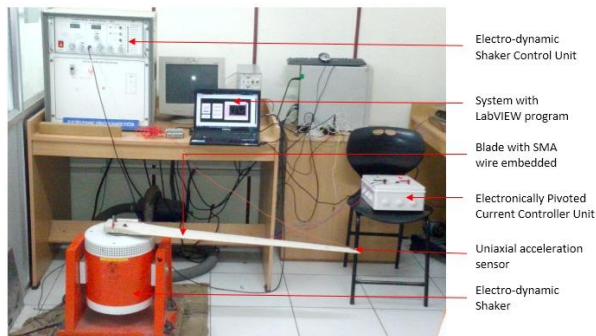


Fig. 7 Experimental setup for active vibration control in SMA embedded blade

pass the acceleration signal to the current controller unit, which in turn generates the necessary current for the corresponding displacement incurred in the blade via LabVIEW program installed in the personal computer.

The electro-dynamic controller unit was used to set the frequency and amplitude manually, thereby the electro-dynamic shaker table with the SMA embedded blade mounted was subjected to flapwise vibrations.

## 6. Comparison of Passive and Active Vibration Control of Smart Blade

With respect to the experimental setup shown in the previous section, the harmonic response of conventional and smart blade was compared in Fig. 7, shown below.

Passively the SMA wires, without any supply of current, has produced a 20% increase in frequency and reduction in displacement of 21.3%, compared to the conventional blade. Using the active supply of current from the electronically pilot current controller kit, the displacement of the smart blade has been reduced to 4.21mm.

It can be observed that, at all frequencies, there was a significant reduction in displacement of smart blade in active control of flapwise vibration in SHAWT when compared to passive control of flapwise vibration in SHAWT and blade without SMA. Nearly 61.48% reduction in displacement occurs at the first mode of the natural frequency of smart blade in active control of flapwise vibration compared to conventional blade.

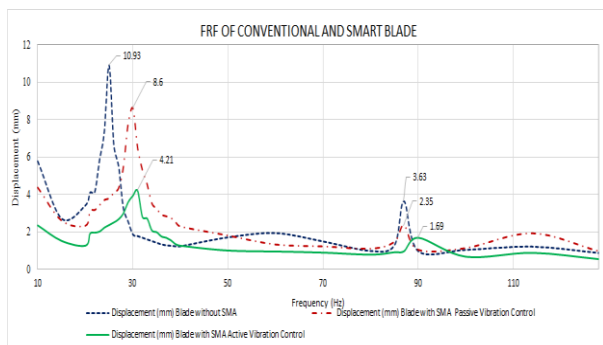


Fig. 8 Comparison of passive and active vibration control of smart blade

Displacement was reduced to 51.04% at the first mode of the natural frequency of smart blade in active control of flapwise vibration compared to passive control of flapwise vibration, depicting the effect of actuation provided by the current control unit on smart blade.

## 7. Conclusions

On embedment of 0.073% of SMA into the wind turbine blade, the smart blade passively and actively depicted an increase in frequency and reduction in amplitude of vibration in the harmonic analysis.

In passive vibration control,

- The 20% increase in frequency of the smart blade is due to modulus of SMA wire being higher than that of glass fibre.
- The 20% reduction in amplitude of vibration is due to the super elastic nature of the shape memory alloy.
- The increase in stiffness of the blade, will also improve the structural integrity of the blade system.

In active vibration control,

- With supply of current on basis of the empirical relation between displacement and current, the smart blade induces increase in the natural frequency of the passive blade.
- As the recovery stress of the SMA increases, with supply of current, the reduction in amplitude of vibration of 51% is depicted in the analysis.
- With thermal expansion of SMA wires, the internal compressive stress of the blade increases, thereby increasing the natural frequency of the smart blade by 3%.
- Significant reduction in the amplitude of vibration at all frequency is depicted, which is due to the increase in the recovery stress of the embedded SMA wires.

Even though the embedment of SMA wires improves the vibration characteristics of the conventional blade, the cyclic increase and decrease in the compressive stress of the blade may result reduction in fatigue properties of the blade. Hence a detailed analysis has to be performed on the fatigue and creep characteristics of the smart blade, to determine the life of the blade at dynamic conditions.

## Acknowledgments

The authors would like to acknowledge Ministry of New and Renewable Energy (MNRE) India and PSG college of technology who have supported at various stages of this reported work.

## References

- Aoki, T. and Shimamoto, A. (2004), "Active vibration control using cantilever beam of smart matrix composite with

- embedded shape memory alloy”, *Key Eng. Mater.*, **270**. Trans Tech Publications.
- Arrigan, J., Pakrashi, V., Basu, B. and Nagarajaiah, S. (2011), “Control of flapwise vibrations in wind turbine blades using semi-active tuned mass dampers”, *Struct. Control Health Monit.*, **18**(8), 840-851.
- Bhargaw, H.N., Ahmed, M. and Sinha, P. (2013), “Thermo-electric behaviour of NiTi shape memory alloy”, *T. Nonferrous Metals Soc. China*, **23**(8), 2329-2335.
- Gupta, K., Sawhney, S., Jain, S.K. and Darpe, A.K. (2003), “Stiffness characteristics of fibre-reinforced composite shaft embedded with shape memory alloy wires”, *Defence Sci. J.*, **53**(2), 167.
- Jovanović, M.M., Simonović, A.M., Zorić, N.D., Lukić, N.S., Stupar, S.N. and Ilić, S.S. (2013), “Experimental studies on active vibration control of a smart composite beam using a PID controller”, *Smart Mater. Struct.*, **22**(11), 115038.
- Khot, S.M., *et al.* (2012), “Active vibration control of cantilever beam by using PID based output feedback controller”, *J. Vib. Control*, **18**(3), 366-372.
- Lee, J.W., Kim, J.K., Han, J.H. and Shin, H.K. (2013), “Active load control for wind turbine blades using trailing edge flap”, *Wind Struct.*, **16**(3), 263-278.
- Lim, Y.H. (2003), “Finite-element simulation of closed loop vibration control of a smart plate under transient loading”, *Smart Mater. Struct.*, **12**(2), 272.
- Lin, Y.J., Lee, T., Choi, B. and Saravanos, D. (1999), “An application of smart-structure technology to rotor blade tip vibration control”, *J. Vib. Control*, **5**(4), 639-658.
- Mani, Y. and Senthilkumar, M. (2013), “Smart material (SMA)-based actively tuned dynamic vibration absorber for vibration control in real time applications”, *J. Eng. Technol.*, **3**(2), 90-96.
- Mani, Y. and Senthilkumar, M. (2015), “Shape memory alloy-based adaptive-passive dynamic vibration absorber for vibration control in piping applications”, *J. Vib. Control*, **21**(9), 1838-1847.
- Mollasalehi, E., Wood, D.H. and Sun, Q. (2012), “Small wind turbine tower structural vibration”, *Proceedings of the ASME IMECE*, Houston, TX.
- Qiao, Y., Han, J., Zhang, C. and Chen, J. (2012), “Modeling smart structure of wind turbine blade”, *Appl. Compos. Mater.*, **19**(3-4), 491-498.
- Qiu, Z. (2015), “Experiments on vibration suppression for a piezoelectric flexible cantilever plate using nonlinear controllers”, *J. Vib. Control*, **21**(2), 300-319.
- Quek, S.T., Wang, S.Y. and Ang, K.K. (2003), “Vibration control of composite plates via optimal placement of piezoelectric patches”, *J. Intel. Mat. Syst. Str.*, **14**(4-5), 229-245.
- Saad, M.S., Jamaluddin, H. and Mat Darus, I.Z. (2015), “Online monitoring and self-tuning control using pole placement method for active vibration control of a flexible beam”, *J. Vib. Control*, **21**(3), 449-460.
- Sanusi, K.O., Ayodele, O.L. and Khan, M.T.E. (2014), “A concise review of the applications of NiTi shape-memory alloys in composite materials”, *South African J. Sci.*, **110**(7-8), 1-5.
- Sellami, T., Berriri, H., Darcherif, A.M., Jelassi, M. and Mimouni, M.F. (2016), “Modal and harmonic analysis of three-dimensional wind turbine models”, *Wind Eng.*, **40**(6), 518-527.
- Singh, S.P., Pruthi, H.S. and Agarwal, V.P. (2003), “Efficient modal control strategies for active control of vibrations”, *J. Sound Vib.*, **262**(3), 563-575.
- Tushar, C. and Mukesh, S. (2014), “Experimental vibration analysis of piezo-laminated beam”, *Int. Res. J. Sci. Eng.*, **2**(3), 94-99.
- Xu, S.X. and Koko, T.S. (2004), “Finite element analysis and design of actively controlled piezoelectric smart structures”, *Finite Elem. Anal. Des.*, **40**(3), 241-262.
- Yuvaraja, M. and Senthilkumar, M. (2013), “Comparative study on vibration characteristics of a flexible GFRP composite beam using SMA and PZT actuators”, *Procedia Eng.*, **64**, 571-581.

HJ